Atmos. Chem. Phys. Discuss., 11, C14515–C14524, 2012
www.atmos-chem-phys-discuss.net/11/C14515/2012/

Atmospheric Chemistry and Physics Discussions

Interactive comment on "Birch and conifer pollen are efficient atmospheric ice nuclei" *by* B. G. Pummer et al.

C Zetzsch

cornelius.zetzsch@uni-bayreuth.de

Received and published: 19 January 2012

Expansion cooling improves the capabilities of our LOw-Temperature Aerosol Simulation Chamber (LOTASC), described in detail on the homepage of the infrastructure network EUROCHAMP (www.eurochamp.org). The depolarization detector (DPD) enables us to detect particles by backscattering of laser light and to identify anisotropic optical properties of the particles, such as ice nucleation, from depolarization. We feel that the new properties of the facility, the experimental procedure of this study and relevant results should be illustrated and described here in greater detail.

The DPD has been constructed based on a similar instrument (SIMONE), developed previously at the Institute for Meteorology and Climate Research (IMK-AAF) at the Karlsruhe Institute of Technology (KIT), see Büttner (2004), Wagner et al. (2006) and

Möhler et al. (2008). Our instrument rotates a linear polarizer with a speed of typically 10-15 rpm in front of the photomultiplier (Hamamatsu R374). It observes the backscattered light at an angle of 175° with respect to the laser beam (Acculase LC, 635 nm, 5 mW) that disappears in a Wood's horn after traversing the chamber horizontally. The sinusoidal scattering signal varies between $I_{parallel}$ and $I_{orthogonal}$. Taking the total backscattered signal I_{bs} as $I_{parallel}$ + $I_{orthogonal}$ and by determining the amplitude from each minimum and maximum by a real time LabView application, the orthogonal portion, is obtained from the ratio $I_{orthogonal}/I_{bs}$.

The simulation chamber, described by Behnke et al. (1988) as a photochemical smog chamber, is a vertical cylinder with an inner diameter of 1 m that has been extended to a height of 4 m at Bayreuth. It is made of borosilicate glass (Schott, Duran 50) and has been sealed during the joint campaign with Vienna University of Technology of the present study by flat end plates (PVC, 5 cm) for expansion cooling. It is installed in a walk-in room that can be cooled to 248 K. Evacuating the chamber by a 100 m^3/h-pump (Rietschle VFE 101) leads to further cooling of the gas phase in the chamber due to expansion of the gas, depending on humidity and pumping speed. Pressure is measured by a MKS 222 BHS-D-D-1000 transducer, calibrated at atmospheric pressure against an Hg barometer (Gebr. Lambrecht).

The temperature, T_{wall}, of the glass wall and the relative humidity (RH) are determined by a combined T/RH sensor (DKRF 4001-P, Driesen und Kern), calibrated by saturated salt solutions. The sensor for T_{wall} is fixed in a glass joint close to the wall 1.5 m above the sensor for the gas temperature (T_{gas}), that is measured close to the axis of the glass cylinder and is fixed to the end of a glass tube, reaching 40 cm into the chamber (i.e. 10 cm from the axis).The laser beam of the DPD enters the chamber 90 cm below (50 cm above the bottom of the chamber). The sensor for T_{gas} is a centigrade temperature sensor (LM 35C, National Semiconductor), and its deviation from a calibrated Hg thermometer between -30 and +25°C was observed to be up to +/- 0.8 K (requiring a recalibration by a PT100 sensor with better accuracy and resolution).

The response time constant of the LM35C is several seconds and depends on air turbulence, so this needs to be considered in the rapid temperature decrease induced by the sudden pressure drop. An expansion cooling experiment with wet pollen from hazel at ice-saturated humidity is displayed in Figure 1.

Figure 1: Time profiles of the pressure, P_{obs} (left hand logarithmic scale) and gas temperature ($T_{wet,obs}$, $T_{dry,obs}$, right hand linear scale), in two expansion cooling experiments at different humidity and evacuation speed. The dashed lines refer to a measurement with hazel pollen. The red solid curve, $T_{dry,diab,obs}$(measured at room temperature), has been shifted by – 40K to match the start temperature of the hazel experiment. The green line ($T_{dry,adiab}$, dash-dotted) shows the adiabatic temperature change expected for dry adiabatic expansion according to the pressure (blue solid line). The pink curve ($T_{wet,mod}$, dash-dotted) shows a non-adiabatic model calculation (considering heat exchange with the walls and decreasing heat content of the gas with decreasing pressure, see text) fitted to the measured curve for hazel, $T_{wet,obs}$.

The gas temperature, T_{obs}, starts at 254.5 K, about 1 K below the wall temperature (not shown), indicating a minor vertical temperature gradient in the refrigerated room. Upon evacuation at t = 0, the pressure drops almost exponentially to 400 mbar after 225 s. The wall temperature decreases by only about 1 K during this time span, whereas the gas temperature ($T_{wet,obs}$, dashed curve) decreases rapidly to a minimum value of 243 K. According to the Poisson equation for dry adiabatic expansion, the decrease of temperature should occur simultaneously with the pressure drop ($T_{dry,adiab}$, dash-dotted line). The observed $T_{wet,obs}$ is not only delayed by the response time but also by a condensation of humidity on the surface of the sensor. This can be seen by a comparison with dry air ($T_{dry,diab,obs}$, solid curve), where the convex start of the temperature decrease is much less pronounced. Here the response of the sensor causes a delay of about 10 s and then continues almost in parallel to the slightly concave dry adiabatic calculation. (Poisson equation, not considering heat exchange) until heat exchange predominates in the experiment, leading to a minimum.

The observed time profiles in figure 1 approach minima after 110 s (dry) and 200 s (wet), so they deviate strongly from adiabatic expansion. This indicates an influence of heat exchange, increasing with temperature difference between wall and gas, becoming predominant with vanishing gas density. As an attempt to quantify this heat exchange, the expansion chamber and the temperature sensor were further tested: Stopping the evacuation led to an immediate, fairly exponential increase of temperature, approaching the wall temperature with a typical time constant of less than 2 min. Evacuating the dry chamber from atmospheric pressure at room temperature to 200 hPa within 300 s (as partly shown in figure 1) we observed a maximum temperature decrease of 14 K, followed by an increase with an exponential rise-time of about 500 s. This demonstrates clearly that heat exchange between the walls and the gas and the decreasing heat content of the gas, decreasing with pressure, need to be taken into account. On the other hand, detailed dynamic model calculations of non-adiabatic expansion cooling are beyond the scope of this first measurement campaign.

A next question will be how to consider the latent heat of H_2O condensing to liquid water and ice in our system and even more so condensing on the temperature sensor, as indicated by the observed delay of about 20 s in figure 1. This condensation results in the pronounced convex curvature, before the temperature reading drops in the steep fashion expected from the decrease of pressure. An integration of the differential equation relevant to the dimensions of the LOTASC chamber was fitted by adjusting the parameters to the measurement with hazel pollen, $T_{wet,obs}$ in figure 1, and is shown for comparison as $T_{wet,mod}$. The difference of the curves decreases with time and becomes smaller than 0.5 K above 60 s, so we trust in the temperature reading of nucleation with hazel pollen that occurred at 244 K after 160 s This situation was different for birch pollen (our very first experiments), where freezing was observed already 40 s after starting the pump. According to Figure 2 we estimate a difference of about 1.6 K between measurement and model. On the other hand, the few expansion chamber experiments and the uncertainty of the model calculation do not justify a quantitative correction.

Figure 2: Expansion experiment with birch pollen. The difference between the measured and the modeled temperature is about 1.6 K at 40 s, where T_{50} in the manuscript by Pummer et al. has been taken from the measured curve. Note, that the model has been simply adjusted to fit the final decay of the observed temperature.

Another important topic is the short residence time of coarse particles, enclosed in simulation chambers. This residence time is known to decrease rapidly with increasing diameter according to the Stokes law. The residence times of particles in the suspended state have been investigated in detail by Crump and Seinfeld (1981) and Holländer et al. (1984). An extrapolated residence time of 2 h was obtained in the 3-m version of our chamber at a particle diameter of 3 μm from experiments with commercial spherical particles, made of polystyrene (Behnke et al., 1988). The typical settling speed of pollen limits the observation time in our 4 m-chamber, since values of 1.57 cm/s for birch pollen (Kohler et al., 2007) and 21 – 32 cm/s for corn pollen (Aylor, 2002) have been reported for example. Experiments with complete pollen from corn are not feasible in our chamber, as follows from the large diameter (see Table 1 of the paper submitted by Pummer et al.), and grinding of all pollen to smaller diameters was required for the LOTASC runs. Different from the pollen, the commercial protein Snomax^{TM} from *Pseudomonas syringae* bacteria was found to be water suspendable and was atomized directly from aqueous suspensions (at an initial concentration of 1g/L).

We used an impinger mounted on an ultrasonic nebulizer (Quick-Ohm QUV-HEV FT25/16-A), passing the aerosol through 20 cm Teflon tubing with 4 mm inner diameter (both heated to ca. 20°C) into the LOTASC simulation chamber and obtained a mean dry particle diameter around 200 nm by this technique, where the very initial diameters of the droplets from the ultrasonic nebulizer are above 1 μm. In our first experiments the dry pollen samples were ground to smaller size in a vibrating mill (Perkin Elmer) for 10 min, and aqueous suspensions, containing 250-500 mg pollen per 30 ml in the simulation chamber experiments, were prepared in a beaker immersed into an ultrasonic

bath (Bandelin Sonorex R225H) for 1 min. In the later experiments extended grinding was performed in a BIO101 FastPrep Cell Disrupter (FP120A, Qbiogene) but this procedure caused a temperature rise, damaging the sample and leading to a decrease of T_{50}. However, when using the vibrating mill, the thermal decomposition was prevented. Snomax and the pollen from birch and ragweed were prepared with artificial cloud water (following a recipe for typical forest throughfall in the Solling mountainous area by Alewell and Matzner, 1993) during the joint experiments with TU Vienna, the other pollen samples (juniper I, redtop, hazel, plane tree) – investigated by us alone – were treated with bidistilled water. However, the chosen water quality (distilled or artificial rain water) had no significant impact on the nucleation temperature. The suspensions were then dispersed into the LOTASC chamber by the ultrasonic nebulizer, the aerosol filling of the chamber taking again about half an hour, as observed by the increase of the backscattered intensity.

Chamber runs were started by filling first with purified air at a relative humidity of 80% at room temperature. Then the chamber was cooled to the desired starting temperature of the expansion cooling. The surplus of water condensed and froze on the walls (except for the heated observation window of the DPD), thus providing a saturated atmosphere with respect to ice. Then the biological particles were dispersed within the mentioned half an hour at this desired starting temperature to obtain a sufficient particle density. Part of the backscattered intensity, I_{bs}, at t = 0 – 25 s is caused by the pollen. Upon evacuation cooling, supercooled water condenses on the pollen, and growth and increasing number of pollen-activated droplets cause a broad maximum around 100 s. The depolarized fraction remains small during this time period, indicating that this backscattering is due to droplets. After 120 s, it increases suddenly and reaches a final value of about 0.35 after 150 s. The gas temperature, T_{gas}, at the half height of the step is then taken to be the T_{50} value in table 1 of the submitted paper. After the ice nucleation event of interest, the backscattering indicates a slow, continued settling of remaining pollen in the chamber.

We would like to mention here the review by Möhler et al. (2007) on the role of biological particles in cloud physics, summarizing the available studies on pollen, and the still fairly high ice nucleation temperatures observed for birch pollen in the present study. Expansion experiments with Snomax^{TM} aerosol have also been performed in the much larger AIDA chamber (Möhler et al., 2008), resulting in ice nucleation temperatures of 267.5 K (1% of the Snomax cells inducing immersion freezing) without expansion cooling and 265 K with expansion cooling (20% of the Snomax cells active). Recent further experiments in the LOTASC facility with bidistilled water delivered values between 267 and 265 K.

Acknowledgements We wish to thank Martin Schnaiter (IMK-AAF, Karlsruhe) for advice in the construction of the depolarization detector and for making the PhD thesis of Simone Büttner available and Bernhard Pummer and Fabian Weiss (TU Vienna) for participating in the first half of the experiments (transnational access campaign in 2010 within EUROCHAMP-2).

Alewell, C., Matzner, E., Reversibility of soil solution acidity and of sulfate retention in acid forest soils. Water, Air and Soil Pollution, 71, 155-165, 1993.

Aylor, D.E. Settling speed of corn (Zea mays) pollen. Aerosol Science, 33, 1601-1607, 2002. Behnke, W., Holländer, W., Koch, W., Nolting, F., Zetzsch, C.: A smog chamber for studies of the photochemical degradation of chemicals in the presence of aerosols. Atmos Environ., 22, 1113-1120, 1988.

Büttner, S. Streulichtexperimente an asphärischen Aerosolpartikeln: Depolarisationund Vorwärtsstreuverhältnis von Mineralstaub und Eiskristallen. PhD thesis, University of Karlsruhe, 2004, see http://www.imk-aaf.kit.edu/downloads/dissSB.pdf

Crump J. G., Seinfeld J. H. Turbulent deposition and gravitational sedimentation of an aerosol in a vessel of arbitrary shape. J. Aerosol Sci. 12, 405-415, 1981.

Holländer W., Behnke W., Koch W. and Pohlmann G. Design and performance of an

aerosol reactor for photochemical studies. Proc. Third Eur. Symp. Physico-Chemical Behaviour of Atmospheric Pollutants (ed. Versino B. and Angeletti G.), pp. 309-319. D.

Reidel, Dordrecht, 1984. Kohler, F., Schultz, E., Helm, H. Study of morphology and settling velocity of airborne pollen captured in a Paul trap. Abstr. European Aerosol Conference 2007, Salzburg, Abstract T04A028.

Möhler, O., DeMott, P.J., Vali, G., Levin, Z. Microbiology and atmospheric processes: the role of biological particles in cloud physics, Biogeosciences, 4, 1059-1071, 2007.

Möhler, O., Georgakopoulos, D.G., Morris, C.E., Benz, S., Ebert, V., Hunsmann, S., Saathoff, H., Schnaiter, M. and Wagner, R. Heterogeneous ice nucleation activity of bacteria: new laboratory experiments at simulated cloud conditions. Biogeosciences, 5, 1425-1435, 2008.

Wagner, R., Benz, S., Möhler, O., Saathoff, H., Schurath, U. Probing ice clouds by broadband mid-infrared extinction spectroscopy: case studies from ice nucleation experiments in the AIDA aerosol and cloud chamber. Atm. Chem. Phys., 6, 4775-4800, 2006.

Interactive comment on Atmos. Chem. Phys. Discuss., 11, 27219, 2011.

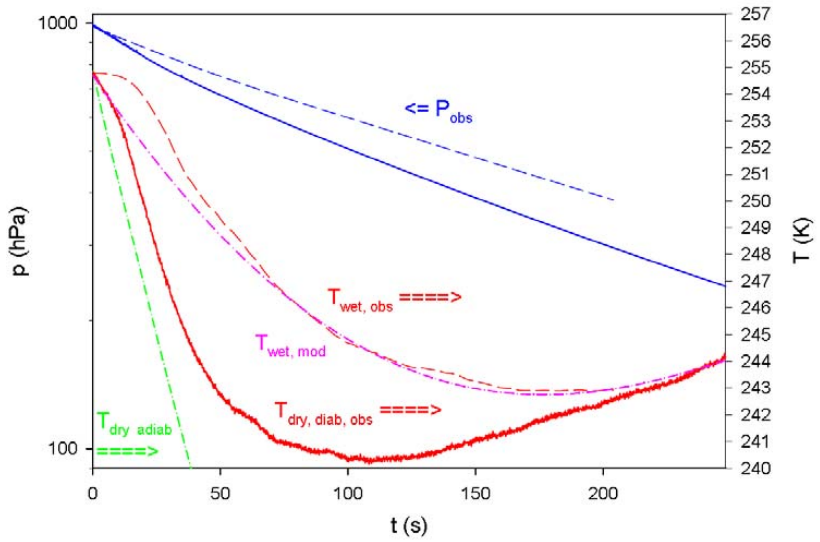

Fig. 1. Time profiles of pressure and temperature for hazel pollen incl. model of expansion cooling (see complete caption in text above)

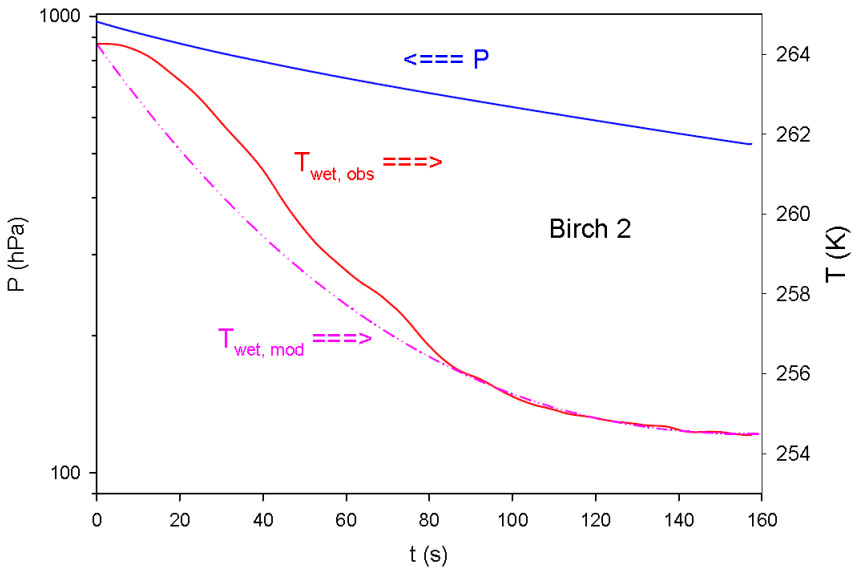

Fig. 2. Time profiles of pressure and temperature for birch pollen incl. model of expansion cooling (see complete caption in text above)